Wave-Optics Analysis of HF Propagation through Traveling Ionospheric Disturbances and Developing Plasma Bubbles

Charles S. Carrano[(1)], John M. Retterer[(1)], Keith M. Groves[(1)], Geoff Crowley[(2)], Timothy M. Duly[(2)†], & Donald E. Hunton[(2)]

(1) Institute for Scientific Research, Boston College
Chestnut Hill, MA, USA 02467

(2) Atmospheric and Space Technology Research Associates LLC
Boulder, CO, United States

Abstract

We apply a wave-optics technique to model the propagation of high-frequency (HF) waves through simulated traveling ionospheric disturbances (TIDs) and developing plasma bubbles at low latitudes. Wave-optics is derived from a forward-propagation approximation of the Helmholtz equation governing the electric field in the frequency domain. The technique is implemented using the split-step Fourier approach commonly referred to as the multiple phase screen method (MPS). At an intermediate step in the computation, the electric field along each phase screen is expressed explicitly in terms of the angular spectrum of plane waves intersecting the screen.

We use this approach to produce angle-of-arrival "maps," which depict the spectrum of angle-of-arrival (AOA) at all locations on the ground. These AOA maps identify all radio propagation modes reaching the receiver along with their individual amplitudes. With the wave-optics approach there is no need to 'home' rays to identify the propagation modes that are present. A full-wave technique, wave-optics accurately represents the interaction (via diffraction) between the different propagation modes, which can result in fading of the received HF signal. Ray-tracing techniques neglect diffraction and therefore cannot represent these interactions nor the signal fading they produce.

1 Introduction

A highly accurate treatment of radio propagation through an inhomogeneous plasma consists of solving Maxwell's equations coupled with the equations of motion for the particles comprising the plasma. The finite-difference-time-domain (FDTD) approach has been applied to solve this problem [1], [2] but requires very high resolution (10-20 samples per wavelength). In long-range communication and over-the-horizon radar (OTHR) applications, the waves interact with the plasma over a distance several orders of magnitude longer than the wavelength, such that the sampling requirements become untenable.

We employ a wave-optics approach that enables efficient HF propagation modeling over long distances in the ionosphere [3]. The wave-optics technique is derived from a forward-propagation approximation of the Helmholtz equation governing the electric field in the frequency domain. It is implemented using the split-step Fourier approach commonly referred to as the multiple phase screen method (MPS). MPS simulations of vertical and oblique HF propagation have been performed by Kiang and Liu [4] and Wagen and Yeh [5], respectively, using a small number of horizontally oriented screens. Hocke and Igarashi [3] used a vertically oriented screens to model HF propagation for an over the horizon radar (OTHR).

An advantage of wave-optics is that relatively large spatial steps (10–100s of wavelengths) may be taken in the direction of propagation. At an intermediate stage of the computation, the electric field along each screen is expressed explicitly in terms of the angular spectrum of plane waves intersecting that screen. From this angular spectrum it is straightforward to determine the amplitude and direction of all propagation modes anywhere in the computational domain. A windowing function is applied to the field surrounding the region of interest to improve localization in space and to suppress side-lobes. From this information we produce angle-of-arrival "maps," which depict the spectrum of angle-of-arrival (AOA) at all locations on the ground. These AOA maps identify all radio propagation modes reaching the receiver along with their individual amplitudes.

2 Simulation of TIDs and Developing Bubbles

In 2010, ASTRA set up a TIDDBIT system near Lima, Peru as part of a campaign to measure TIDs in the upper atmosphere near the geomagnetic equator. The central receiver was located at Ancon and the three transmitters were sited approximately 75 km away at Canta, Lurin, and Huaral. The TIDDBIT instrument is a multistatic ionospheric sounder that measures Doppler shifts in the HF waves reflected from the bottomside ionosphere. From these data, the frequencies, velocities, propagation directions, phases, and amplitudes of the TID waves can be calculated [6]. The system operated from mid November 2010 until mid-September 2012 during which time a large volume of data were collected. We selected data from 20

---

† Now at Spire Global, Inc.

Nov, 2010 for analysis because of coincident turbulence measured by the nearby JULIA radar at Jicamarca, Peru.

PBMOD, the Physics-Based Scintillation Forecast Model [7] is a first principles model of the ionosphere that describes the state of the near-Earth plasma environment from the global scale down to waves of kilometer size. We used PBMOD, driven by the spectrum of neutral-wind modes determined from the TIDDBIT data, to simulate the development of TIDs which seed the Rayleigh-Taylor instability and produce plasma-density irregularities (plasma bubbles). Neutral wind fields were extracted from the TID data using the Hooke ion continuity model. The neutral wind perturbation decreases exponentially above a dissipation altitude (determined within the PBMOD model). The neutral scale height was calculated using climatological models, including MSIS.

The results of using this TID data to initialize and drive the development of plasma structure using PBMOD is shown in Figure 1. The simulation used a 256 by 256 grid in the equatorial plane with a grid-cell size of about 4.5 km square in those dimensions and a comparable number of points along the geomagnetic field lines. Each panel in the figure shows an east-west vertical slice through the ionosphere along the geomagnetic equator. The panels show four times in the development an hour apart. The left panel shows the unstructured, flat ionosphere at the beginning of the simulation. One hour later (second panel) the structured wind fields associated with the measured TIDs have generated bottomside corrugations in the electron density. Signatures of the same ripples can be seen higher in the ionosphere in the F peak altitude range near 400 km. An additional hour later (the third panel) spread-F plumes have formed and by the fourth hour (last panel) the plumes are mature, with density depleted regions reaching through the F-peak into the topside ionosphere. Secondary structure in the walls of the plumes can also be seen. These smaller irregularities are formed by a variety of processes, including the same interchange instability processes that create the primary plume, but on a smaller scale.

3 Wave-Optics Propagation Modeling

We interpolated the 3D gridded electron density data provided by PBMOD onto the plane containing a great circle path oriented in the geographic east-west direction at the midpoint of the data cube, and extended the density field periodically to cover the field of operation of a typical OTHR radar. We then used the wave-optics technique described in [3] to propagate 20 MHz waves through this interpolated density field. The transmitted signal was a spherical wave modulated by a conical antenna gain pattern launched from a hypothetical OTHR situated just outside the computational domain. Ground reflections were imposed by specifying an appropriate refractive index profile beneath the ground surface such that the

waves are reflected in a direction consistent with ray-tracing (as described in [3]). The sampling along each screen was 6.1m, and screens were separated by 0.5 km.

For comparison with the wave-optics result, we also implemented the 2D ray-tracing algorithm by Coleman [8] and traced a fan of rays leaving the transmitter in the directions of high antenna gain (to cover the angular spread of the transmitted beam). The wave-optics and ray-tracing calculations were conducted independently.

Figure 2 below summarizes the results of the HF propagation calculations. The plots in each row correspond to a different time (UT) in the development of the ionospheric structure. The first plot in each row shows a color contour plot of the electron density from PBMOD, depicted in terms of plasma frequency. The second plot in each row shows a color contour plot of signal intensity, obtained from the wave-optics calculation. Superimposed on the intensity plots are white rays that have been explicitly traced from the transmitter. Line-contours of plasma frequency are superimposed on these plots for convenience. The third plot in each row shows a color contour plot of the spectrum of arrival angle. These angle of arrival 'maps' show the locus of all directions from which incident waves are arriving and reflected waves are departing at each point on the ground. The arrival angle is depicted in terms of the local elevation angle while facing toward the receiver, such that incident rays have positive elevation angles and reflected rays have negative elevation angles. The AOA data are colored by spectral power, which indicates the magnitude of the contribution to the total received power from waves travelling in each direction. Red indicates the highest spectral power, while blue indicates the lowest. White dots shown on the maps indicate the footprints on the ground for each traced ray that returns to the surface (not all launched rays return to Earth). The direction of the departing (reflecting) rays are also shown, to facilitate comparison with the wave-optics result.

The evolution of the ionospheric structuring during this event can be seen by the sequence of plots from Figure 2 in the first column, starting from top to bottom. At the first time shown (24 minutes before midnight), the ionosphere is mostly quiescent with only a nascent signature of TIDs developing in response to forcing by the neutral winds. The wave-optics and ray-tracing calculations both predict single-mode propagation to ranges past 2000 km, while the wave-optics calculations also reveal a region of two-mode propagation (high and low reflections from the F region) at shorter ranges.
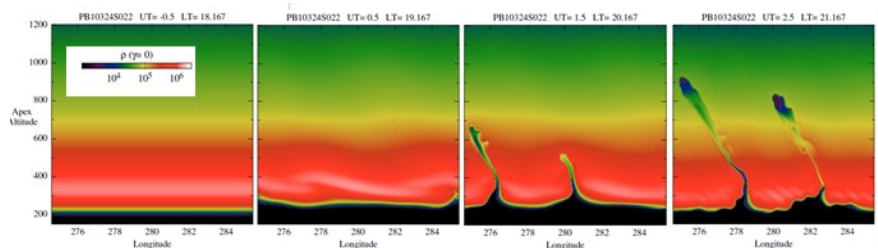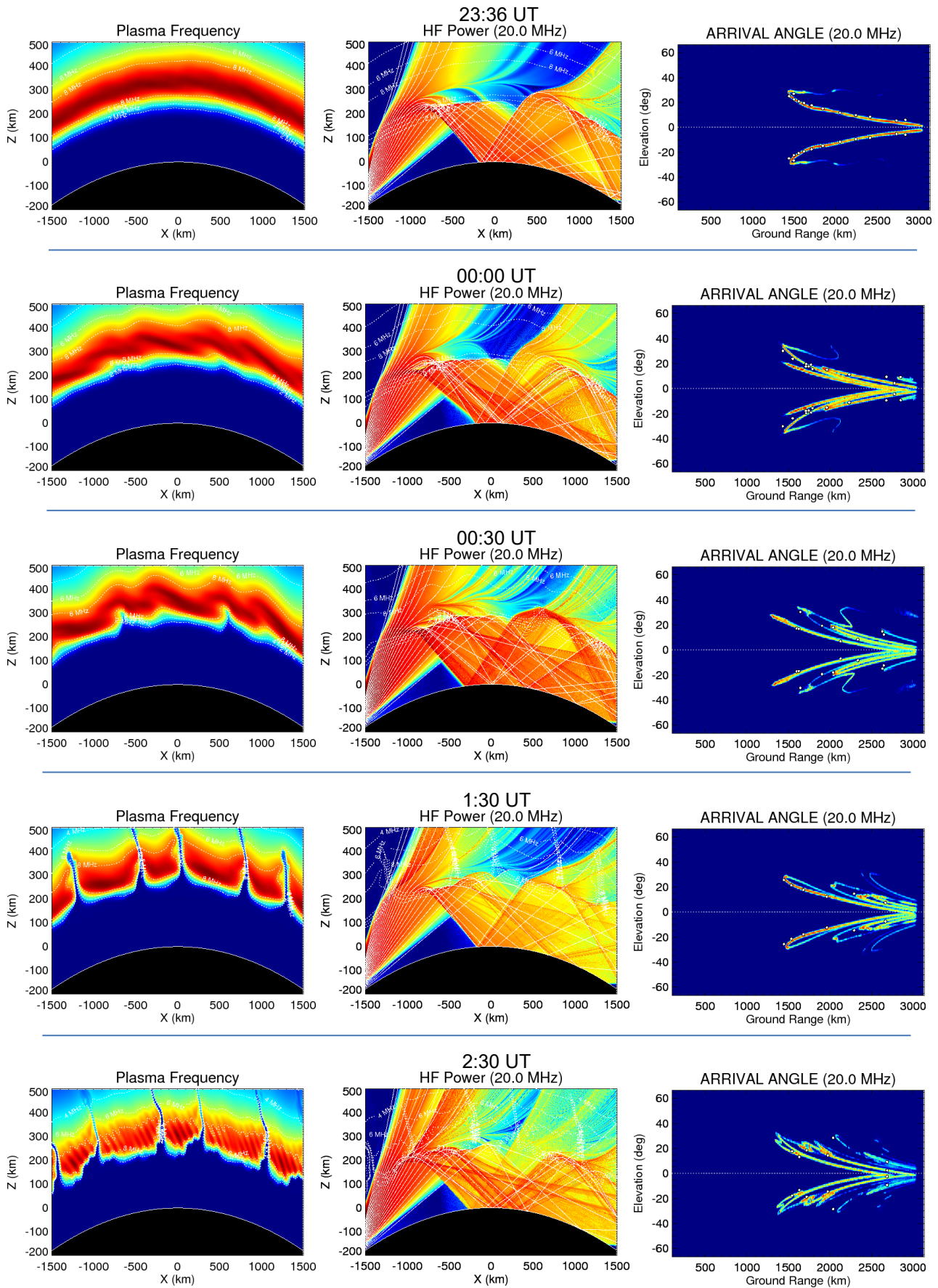

Figure 1. Simulated bubble development from PBMOD.

Figure 2. Plasma frequency (left), HF power (dB) (middle) and arrival angle (right) from wave-optics simulation of a 20 MHz wave propagating through a developing ionospheric disturbance. Color scales are relative with red = high and blue = low.

At the second time shown (midnight), the TIDs have developed and exhibit a significant downward tilt in the zonal direction. Propagation at all ranges is now multi-modal, with at least four distinct modes of propagation present at ranges between 2000-2400 km. Only the wave-optics solution clearly reveals the structure of all propagation modes present. The footprints of the ray-tracing results tend to lie on one of the propagation modes indicated by the wave-optics solution. Without the wave-optics result for comparison, these ray-tracing footprints would appear randomly distributed and difficult to interpret

At the third time shown (30 minutes past midnight) evidence of upward-traveling plumes of low density plasma and downward-traveling plasma enhancements are beginning to develop under the influence of the Rayleigh-Taylor instability. The propagation environment is now highly complex, with at least 7 modes of propagation present at ranges 2100-2300 km. Although it is difficult to discern from the plot, the wave-optics solution predicts some power in the region devoid of rays at short range known as the 'skip zone'. This may be a consequence of the strong caustic that has developed at this time an altitude of about 220 km. The wave optics solution accounts for diffraction, which is able to turn the waves through a larger angle than refraction alone, thus illuminating the ground at closer ranges than predicted by ray tracing.

At the fourth time shown (1:30 UT), the plasma plumes are well developed and the propagation environment becomes more complicated still. Also note that the plumes of depleted plasma begin to act as conduits for HF power to penetrate through the F-region and leak out into space. As a result of this power leakage less power is available to illuminate targets on the ground, thereby reducing the efficiency of the radar.

At the last time shown (2:30 UT), the bottomside ionosphere has undergone further structuring under the influence of secondary instabilities. The propagation environment is the most complex yet, with very many propagation modes present.

4 Discussion and Conclusions

Theory suggests that wave-optics and ray-tracing should predict the same arrival angles under conditions where refractive processes are dominant over diffractive ones. Refractive processes dominate when the scale sizes of plasma irregularities (when present) are much larger than the wavelength (hence the historical success of ray-tracing applications to HF propagation modeling).

The PBMOD simulations herein support structure with scale-sizes of about 10 km. In the absence of sub-grid scale irregularities (which have not been introduced into these simulations), we observed good agreement between wave-optics and ray-tracing results, except in regions of strong focusing following caustics. The wave-optics approach provides significantly more information about the propagation environment than ray-tracing, as both the spectra of wave power and direction are available at any point on the ground. Ray tracing provides only angle information (although a crude estimate of power can also be inferred from the density of rays), and only where the launched rays happen to land. The additional information provided by wave-optics is most useful when the propagation environment is highly multi-modal. Under these conditions the ray-tracing results become difficult to interpret because the ray footprints appear to be distributed randomly. The wave-optics results show that while the propagation environment is complex for these scenarios, it remains deterministic and systematic, with multiple modes of propagation clearly defined for all ranges. We believe the additional information provided by wave-optics can be leveraged to improve OTHR performance.

In a future work, we plan to embed small (sub-grid) scale irregularities within the large scale TID and plume structure. Scattering by these small-scale irregularities should produce diffraction effects that ray-tracing is fundamentally unable to represent. If the irregularity scale sizes with appreciable power approach the wavelength, back-scattering will become significant and the wave-optics formalism will also break down, thereby requiring a more complete treatment via the FDTD method.

5 Acknowledgements

6 References

1. Nickisch, L. & P. Franke (1992), Finite-difference time-domain solution of Maxwell's equations for the dispersive ionosphere, IEEE Antennas Propag. Mag., 34.

2. Yu, Y., J. Niu, & J. Simpson (2012), A 3-D global Earth-ionosphere FDTD model including an anisotropic magnetized plasma ionosphere, IEEE Trans. Antennas Propag., 60.

3. Hocke, K. & K. Igarashi (2003), Wave-optical simulation of the oblique HF radio field, Radio Sci., 38(3), 1039.

4. Kiang, Y.-W. & C. Liu (1985), Multiple phase-screen simulation of wave propagation in the turbulent stratified ionosphere, Radio Sci., 20(3), 652-668.

5. Wagen, J.-F. & K. Yeh (1989), Simulation of HF propagation and angle of arrival in a turbulent ionosphere, Radio Sci., 24, 196–208.

6. Crowley, G. & F. Rodrigues (2012), Characteristics of traveling ionospheric disturbances observed by the TIDDBIT sounder, Radio Sci., 47(4).

7. Retterer, J. (2010), Forecasting Low-Latitude Radio Scintillation with 3-D Ionospheric Plume Models: I. Plume Model, J. Geophys. Res., 115, A03306.

8. Coleman, C. (1998), A ray tracing formulation and its application to some problems in over-the-horizon radar, Radio Sci., 33 (4), 1187-1197.